Journal of Materials Chemistry B

Incorporation of quantum dots in silk biomaterials for fluorescence imaging

Journal:	*Journal of Materials Chemistry B*
Manuscript ID:	TB-ART-02-2015-000326.R1
Article Type:	Paper
Date Submitted by the Author:	09-Jun-2015

Complete List of Authors:	Zheng, Zhaozhu; Soochow University, National Engineering Laboratory for Modern Silk Liu, Meng; Soochow University, Jiangsu Institute of Hematology Guo, Shaozhe; Soochow University, National Engineering Laboratory for Modern Silk Wu, Jianbing; Soochow University, National Engineering Laboratory for Modern Silk Lu, Disi; Heilongjiang University, Li, Gang; Soochow University, National Engineering Laboratory for Modern Silk Liu, Shanshan; Soochow University, National Engineering Laboratory for Modern Silk Wang, Xiaoqin; Tufts University, Kaplan, David; Tufts University, Department of Biomedical Engineering

Incorporation of quantum dots in silk biomaterials for fluorescence imaging

Z.Z. Zheng,[a] M. Liu,[b,#] S.Z. Guo,[a] J.B. Wu,[a] D.S. Lu,[d] G. Li,[a] S.S. Liu,[a] X.Q. Wang,[a*] and D. L. Kaplan[ac**]

a National Engineering Laboratory for Modern Silk, Soochow University, Suzhou, China 215123

b The Cyrus Tang Hematology Center, Jiangsu Institute of Hematology, Soochow University, Suzhou, China 215123

c Department of Biomedical Engineering, Tufts University, Medford, Massachusetts, USA 02155

d College of Chemical Engineering and Material Chemistry, Heilongjiang University, Harbin, China 150086

* Corresponding author: Tel.: +86 512 65883371; fax: +86 512 65883371. 199 Renai Road, Suzhou Industrial Park, Suzhou, Jiangsu Province, P.R. China 215123

E–mail addresses: wangxiaoqin@suda.edu.cn

** Corresponding author. Tel.: +1 617 627 3251; fax: +1 617 627 3231. Departments of Biomedical Engineering and Physics, Tufts University, Medford, Massachusetts, USA 02155

Email address: david.kaplan@tufts.edu

[#] First two authors contributed equally to this work and should be considered co–first authors

Abstract

Tracking the distribution and degradation of biomaterials after *in vivo* implantation or injection is important for tissue engineering and drug delivery. Intrinsic and externally labeled fluorescence has been widely used for these purposes. In the present study, 3-mercaptopropionic acid (MPA)-coated CdTe quantum dots (QDs) were incorporated into silk materials via strong interactions between QDs and silk, likely involving the hydrophobic beta-sheet structures in silk. MPA-QDs were pre-mixed with silk solution, followed by ultrasonication to induce silk gelation or by blending with polyvinyl alcohol (PVA) to generate silk microspheres. Silk structural changes and hydrogel/microsphere morphologies were examined by ATR-FTIR and SEM, respectively. The fluorescence of QDs-incorporated silk hydrogels and microspheres remained stable in PBS pH 7.4 for more than 4 days. The amount of QDs released from the materials during the incubation was dependent on loading; no QDs were released when loading was below 0.026 nmol/mg silk. After subcutaneous injection in mice, the fluorescence of QDs-incorporated silk microspheres was quenched within 24 h, similar to that of free QDs. In contrast, the QDs-incorporated silk hydrogels fluoresced for more than 4 days *in vivo*.

Key words: silk, quantum dots, hydrogel, fluorescence imaging

1. Introduction

Silk is a high molecular weight structural protein derived from the *Bombyx mori* silkworm and has been widely used as a building block to fabricate biomaterials for tissue engineering and drug delivery [1-3]. The amino acid sequence of silk is dominated by Gly–Ala–Gly–Ala–Gly–Ser repeats [4]. Silk molecule consists of a light chain (25 kDa) and a heavy chain (390 kDa) that are linked by a single disulfide bond. Through simple aqueous processing silk can be fabricated into different material formats, such as hydrogels, tubes, sponges, fibers, microspheres and thin films with remarkable mechanical and biological properties [5]. These silk biomaterials can be used as cell-supporting scaffolds in tissue engineering and *in vitro* disease models, or as carriers for drug delivery [6]. Understanding the fate (degradation and organ distribution) of silk biomaterials after implantation or injection *in vivo* is of importance to biomedical applications.

Non–invasive imaging modalities, such as small animal imaging techniques are more preferred than invasive techniques such as immunohistological analyses, because the implants can be evaluated *in situ* and *in vivo* without the need of sacrificing animals. Chemically synthesized organic fluorophores that are used for *in vivo* imaging often encounter problems with fluorescence intensity and stability [7-9]. In addition, fluorophores need to be conjugated to the biomaterials via chemical cross-linking, which can negatively impact material properties. Radioactive labeling of biomaterials has been used to monitor the biodistribution and metabolism of biomaterials, but this is a relatively complicated and challenging procedure, limiting its utility. The use of

nanoparticles for imaging has gained considerable momentum in recent years. Semiconductor nanocrystals, also known as quantum dots (QDs), have gained popularity as a replacement for traditional organic fluorescent markers in biological studies due to their unique optical properties including high quantum yield, size–tunable absorption and emission, improved photostability, broad excitation wavelength range, and narrow emission peak to enable multiplexing labels [9].

QDs have been successfully used in live cell imaging, *in vivo* imaging, and diagnostics [7, 10]. QDs have also been used to label biomaterials to monitor biological distributions and degradation. Biodegradable polymeric vesicles (PLGA-SPION-Mn:ZnS nanoparticles) as nanocarrier systems for multimodal bio-imaging and anticancer drug delivery have been developed and incorporated in vesicles for continuously monitoring uptake by cells for 24 hours [11]. Dual-modal fluorescent–magnetic nanoparticles (FMCPNPs) were developed and *in vivo* fluorescence imaging results suggested that the nanoparticles preferentially accumulated in tumor tissues [12]. Quantum dots conjugated to carbon nanotubes (CNT-QD) were injected into tail veins in mice and emission at 800 nm was monitored in live animals. After circulation for 6 days, strong signals of CNT-QD in several organs of the living animal were still detectable, including liver, kidney, stomach, and intestine [13]. $CuInSe_xSe_{2-x}$/ZnS quantum dots were encapsulated into poly(lactic-co-glycolic acid) (PLGA) microparticles and orally administered to mice, with fluorescence signals tracked in the intestine at 45 h after oral gavage [14].

Silk has become an important biomaterial for biomedical and tissue engineering applications. Until now, non–invasive fluorescence imaging on the degradation and

distribution of silk biomaterials after injection or implantation *in vivo* has not been reported. Silk has been previously used as a stabilizer for coating QDs [15, 16] and QDs have been incorporated into silk fibers for dying [17], but these were not for the purpose of in vivo imaging of silk biomaterials. In the present study, we examined the feasibility of labeling silk biomaterials with QDs via physical entrapment, thereby providing a useful tool for studying silk biodegradation and distribution *in vivo*. The silk biomaterials used were hydrogels prepared by ultrasonication [18] and microspheres prepared with polyvinyl alcohol (PVA) emulsification, as previously reported [19]. Silk hydrogels are soft, flexible and adaptable materials useful as delivery vehicles for bioactive compounds such as drugs and proteins [20, 21], as scaffolds for tissue engineering [22], artificial organs [23], and for sensors [24]. The QDs used in this study were 3-mercaptopropionic acid (MPA) coated CdTe QDs. The fluorescent hydrogels and microspheres were subjected to *in vitro* characterization in terms of fluorescence and material properties and *in vivo* imaging studies after subcutaneous injection in mice.

2. Materials and methods

2.1 Materials and instruments

Partially degummed silk fibers were purchased from Xiehe silk corporation Ltd (Hangzhou, China). Lithium bromide (LiBr) was purchased from Aladdin (Shanghai, China). $Cd(ClO_4)_2 \cdot 6H_2O$, Al_2Te_3 powders, and mercaptopropionic acid (MPA) were purchased from Alfa Aesar (MA, USA). Polyvinyl alcohol (PVA) was purchased from Sigma–Aldrich (St. Louis, MO). Formvar/carbon film coated grids (150 mesh) were purchased from Zhongjingkeyi Technology Co., Ltd (Beijing, China). Human dermal fibroblasts (Hs 865.Sk cells) were obtained from ATCC (American Type Culture

Collection, Maryland, USA). high-glucose Dulbecco's modified Eagle's medium (HG-DMEM), Dulbecco's modified phosphate-buffered saline (D-PBS), Fetal Bovine Serum (FBS) (fatty-acid free) and 0.05% trypsin-0.5 mM EDTA were obtained from GIBCO (Life Technologies, USA). Cell counting Kit-8 (CCK-8) was purchased from Dojindo (Shanghai, China). Other chemical reagents were purchased from Sinopharm chemical reagent co. Ltd (Shanghai, China). Kunming mice (20–25 g) were purchased from SLRC laboratory animal Co. Ltd. (Shanghai, China). The design of the animal experiments was approved by the ethical committee of Soochow University, China. All the animal experiments were performed in compliance with the Guiding Principles for the Care and Use of Laboratory Animals, Soochow University, China. Animals had free access to food and water.

2.2 Synthesis of CdTe QDs

CdTe QDs were prepared by colloidal methods as reported in the literature [25]. Briefly, 0.985 g (2.35 mmol) of $Cd(ClO_4)_2 \cdot 6H_2O$ was added to 125 mL water. To this, 5.7 mmol mercaptopropionic acid (MPA) was added. The pH of the above solution was raised to 11.2 and purged with N_2. The tellurium precursor H_2Te gas was prepared by reaction with 0.2 g (0.46 mmol) of Al_2Te_3 lumps in 15–20 mL of 0.5 M H_2SO_4 under N_2 atmosphere. H_2Te gas was passed through the solution together with a slow nitrogen flow for ~20 min. CdTe precursors were formed at this stage as seen by a change of the solution color. The precursors were converted to CdTe nanocrystals by refluxing the reaction mixture at 100°C. The size of the CdTe QDs grew further with time and was controlled by the duration of reflux; monitored by fluorescence spectroscopy. The newly prepared QDs were precipitated with isopropyl alcohol, and dried in a fume hood and dissolved in water before use [26].

2.3 Purification of silk fibroin

Silk fibroin (hereafter termed silk) was purified by degumming silk fibers in sodium carbonate solution and dissolving in lithium bromide solution as previously reported [6]. Briefly, silk fibers were boiled in 0.02 M sodium carbonate solution for 30 min, rinsed with ultrapure water three times, drained and dried in a fume hood overnight. The dried fibers were dissolved in 9.3 M lithium bromide solution at 60°C for 4 hr to obtain a concentration of 20%. The solution was dialyzed against pure water for 30 h to remove the lithium bromide and centrifuged to remove insoluble fibrous debris. The concentration of purified silk was about 9 wt.%. Higher concentrations of silk were obtained by dialysis against 15% PEG–20000 [27].

2.4 Preparation of QDs incorporated silk microspheres and hydrogel

Silk microspheres were prepared using a PVA emulsification-drying method, as reported previously [19]. Briefly, 1 mL of 10 wt.% silk was mixed with 4 mL of 5 wt.% of PVA in a 15 mL conical tube and the blend solutions were subjected to sonication using an ultrasonic cell disruptor (model JY92–II DX, Scientz) at an energy output of 30% amplitude for 30 s. The solution was immediately transferred to a 55×15 mm diameter petri dish that was placed in a 60℃ oven for 5 hr for drying. The dried silk/PVA films were dissolved in 30 mL of ultrapure water in 50 mL centrifuge tubes for more than 30 min at room temperature. The tubes were centrifuged in a high-speed centrifuge (Beckmann, JX–26) at 5,000 g, 20 min, and 25°C. The supernatant was carefully discarded and the pellet was suspended in 30 mL water for washing. The washing steps were repeated twice to remove residual PVA. The final pellet was suspended in 1 mL of ultrapure water and sonicated at 30% amplitude for 30 sec to disperse the clustered silk spheres. To prepare QD-incorporated silk

microspheres, the dried QDs were dissolved in ultrapure water and the solution was mixed with concentrated (18 wt.%) silk to obtain 10 wt.% silk/QDs solution. The rest of the steps were the same as above.

Silk hydrogels were prepared by ultrasonication–induced methods [18]. One mL of 5 wt.% silk solution was sonicated using an ultrasonifier (JY92–II DX, SCIENTZ, China) with an ultrasonic Φ3 cm probe and ultrasonic energy of 120 W (30% power) for 90 sec. After sonication, the solution was loaded into a 1 mL syringe for *in vitro* and *in vivo* studies. To prepare QD-incorporated silk hydrogels, the dried QDs were re–dissolved in ultrapure water and then mixed with ~9 wt.% silk solution to obtain a final concentration of 5 wt.%. The rest of the preparation steps were the same as above.

2.5 Characterization of silk/QDs hydrogel and microspheres

Silk structure determination by Fourier Transform Infrared Spectroscopy (FTIR)

Silk and silk/QDs hydrogels (200 μL) were prepared in a 24–well plate. The gels were frozen at –80°C overnight and lyophilized for 48 hr in a lyophilizer (Alphk 2-4 LSC plus, Christ, Germany). Silk and silk/QDs microspheres were lyophilized directly. The dried samples (hydrogel and microspheres) were ground into powder together with potassium bromide (KBr), and pressed into discs for FTIR measurement using a Nicolet 5700 spectrophotometer (Thermo, USA). For each measurement, 24 Scans were recorded with a resolution of 4 cm^{-1}, and a wavenumber range of 400-4000 cm^{-1}. Deconvolution of the infrared spectra covering the amide I band (1595-1705 cm^{-1}) was carried out using PeakFit 4.12 (SPSS Inc.). The mode of AutoFit Peaks II Second Derivative was applied to the original spectra in the amide I, and the peak width and

height were adjusted to achieve $R^2 \geq 0.99$. The α-helices and β-sheets contents were obtained by calculating peak areas.

Morphology determination by scanning electron microscope (SEM)

Silk and silk/QDs hydrogels were lyophilized as described above. A piece of the dried hydrogel was mounted on a sample stub using a conductive tape and sputter–coated with Au. SEM images were taken using a Hitachi scanning electron microscope (S–4800, Tokyo, Japan) at 3.0 kV. For silk and silk/QDs microspheres, the powder of dried microspheres was evenly distributed on top of the conductive tape on a sample stub. The samples were subjected to the SEM detection as described above.

QDs determination by transmission electron microscope (TEM)

Silk and silk/QDs hydrogels were lyophilized as described above. A piece of the dried hydrogel was suspended in ultrapure water and sonicated using an ultrasonic cell disruptor (model JY92–II DX, Scientz) at an energy output of 30% amplitude for 3 min to obtain small fragments. The formvar/carbon film-coated grids (150 mesh) were twice dipped into the suspension. Samples were air-dried and then placed in a vacuum oven to completely dry overnight. TEM images were taken using a HITACHI transmission electron microscope (HT7700, Tokyo, Japan). For silk and silk/QDs microspheres, the powder of dried microspheres was disperse in water. The samples were prepared and subjected to the TEM detection as described above.

QDs release from silk hydrogels and microspheres

Silk/QDs hydrogels (200 μL) were prepared in 24–well plates. The QDs loading was 0, 0.013, 0.026, 0.065, 0.13 and 0.26 nmol/mg silk. After the solution gelled, 1 mL of ultrapure water was added to each well, and the samples were incubated at 37°C. The release medium was replenished at 10 min, 0.5, 1, 2, 12, 24, 36, 48, and 60 hr. The fluorescence spectra in the release media were determined by a synergy H1

microplate reader (Bio–Tek, USA) at an excitation wavelength of 380 nm and emission wavelength of 450–700 nm. For silk/QDs-microspheres, the suspension (20 mg/mL) in a 2 mL tube was incubated at 37°C. At 0.5, 1, 2, 12, 24, 36, 48, and 60 hr, the samples were centrifuged using a Thermo high speed centrifuge (Thermo Scientific, LEGEND Micro 21R) at 5,000 rpm, for 10 min. The supernatants were transferred to empty tubes for fluorescence determination as described above, and the pellets were suspended in 2 mL water to continue to study the release.

QDs stability in silk hydrogels and microspheres

Silk/QDs hydrogels (50 μL) were prepared in 96–well cell culture plates. The QDs loading was 0, 0.013, 0.026, 0.065, 0.13 and 0.26 nmol/mg silk. After the solution gelled, 100 μL of ultrapure water or 10 mM PBS (pH 7.4) was added to each well. The samples were incubated at 4°C, room temperature and 37°C. At designated time points (0, 2, 6, 12, 24, 48, 72, 96, 120, 144, 168, and 192 hr), the solution on top of the gel was removed and the gel samples were subjected to fluorescence determination using a synergy H1 microplate reader (Bio–Tek, USA) at excitation wavelength of 380 nm and emission wavelength of 450–700 nm. After measurement, 100 μL of ultrapure water or 10 mM PBS (pH 7.4) was added to each well and the samples were incubated until the next measurement. For silk/QDs microspheres, 100 μL (50 mg/mL) aliquots of microsphere suspension was incubated at 4°C, room temperature and 37°C in a 96–well plate. At designated time points (0, 6, 19, 30, 43, 55, 67, 79, and 91 hr) the samples were subjected to fluorescence determination as described above.

2.6 Cell response on silk/QDs materials

Cell culture

HS 865. SK cells were seeded in 9-cm plates at a density of 7×10^6 cells per dish and cultured with 12 mL high glucose Dulbecco's modified eagle medium (DMEM) supplemented with 10% fetal bovine serum (FBS) (Gibco, Life Technologies, USA) at 37.0 ± 0.2°C in a humidified air incubator containing 5% CO_2. When the cell density reached approximately 80% confluence, the cells were harvested, trypsinized, washed and seeded onto 96-well plates (Corning, USA) with 100 μL cell culture medium each well. Cell seeding density was approximately 3,000 cells per well for silk and silk/QDs hydrogel samples, and 5,000 cells per well for silk and silk/QDs microsphere samples. The number of cells was counted using a VI-CELL XR (Beckman Coulter, USA). After 12 hr culture, cell culture medium was aspirated and different dosage of silk and silk/QDs materials were added. For the silk and silk/QDs hydrogel sample, 20 μL sonicated silk and silk/QDs (0.013, 0.026, 0.065, and 0.13 nmol QDs per mg silk) solutions were added onto cells, incubated for 15 min until silk gelled and formed a thin layer on cells. DMEM containing 10% FBS (100 μL) and 40 μL plain DMEM were added into each well. For free QDs control, 100 μL DMEM containing 10% FBS and 40 μL QDs solution (0.013, 0.026, 0.065, and 0.13 nmol QDs/mL DMEM) were added to each well. For the silk and silk/QDs microspheres, 100 μL DMEM containing 10% FBS and 40 μL (3.33 mg/mL) silk and silk/QDs microsphere suspension (0.013, 0.026, 0.065, and 0.13 nmol QDs/mg silk) were added into cell. For free QDs control, 100 μL DMEM containing 10% FBS and 40 μL QDs solution (0.0043, 0.0087, 0.022, and 0.043 nmol QDs /mL DMEM) were added into eachcells.

Cell viability

Cell counting was achieved using kit-8 (CCK-8, Dojindo, Shanghai, China) with a working mechanism similar to methylthiazol tetrazolium (MTT) assays [28]. For determination of cell viability, the cells were cultured for 0, 24, 48 hr, washed with D-Hanks buffer solution and incubated in 154 μL fresh cell culture medium containing 14 μL CCK-8 solution (5 mg/mL) for 2 h. Thereafter, 100 μL cell culture medium was transfer to a new 96-well plate. The absorbance was measured at 450 nm using a microplate reader (Bio-TEK instrument, USA).

Microscopic observation

The cells after CCK-8 testing were washed twice with PBS buffer, pH 7.4, incubated in 50 μL serum-free culture medium supplemented with 1.87 ng/mL calcium AM (Dojindo, Shanghai, China) for 20 min at 37°C, and observed under the fluorescence microscope (Axio Vert.A1, Carl Zeiss, Germany).

2.7 In vivo assessments of Silk/QDs microspheres and hydrogels

Subcutaneous injection

Mice weighing 20~25 grams were used for the experiment. They were randomly assigned to 5 groups with 3 mice each group (n = 3) as follows: silk/QDs hydrogel, silk hydrogel, silk/QDs microspheres, silk microspheres, QDs solution (control). Before subcutaneous injection, the hair on the backs was removed. Silk/QDs hydrogels or microsphere solutions at a concentration of 5 wt.% were loaded in 1 mL syringes, and 300 μL was dosed by single subcutaneous injections in the back using an 18–gauge needle. The QDs loading was 0.065 nmol/mg silk in the microspheres and hydrogels. After dosing, all rats were placed back in their cages.

Fluorescence imaging

In vivo small–animal imaging was performed every 24 hr using a Caliper IVIS Lumina II system (Caliper Life Sciences, USA). The exposure time (1 sec), excitation filter (500 nm), and emission filter (DsRed) were set prior to detection. The images were recorded at 0, 24, 48, 72 and 96 hr for the mice injected with silk/QDs hydrogels and microspheres.

Statistical analysis

Data were analyzed by two-way ANOVA. Statistical significance was set as p values less than 0.05.

3 Results and Discussion

3.1 Incorporation of QDs in silk hydrogel and microspheres

The cores of the QDs were synthesized in water and capped with thiol–containing molecules (MPA). Photophysical properties of the MPA-capped QDs before and after incorporation in silk hydrogels and microspheres were investigated. Under UV (365 nm) the silk/QDs hydrogels and microspheres strongly fluoresced. Figure 1A shows images of free QDs and QDs-incorporated silk hydrogels, as well as fluorescence spectra for these samples. The emission wavelength of MPA–capped QDs peaked at 595 nm (red fluorescence). At this fluorescence emission wavelength, the size of the MPA-capped QDs should be 3.13 nm [29]. The fluorescence emission of QDs-incorporated silk hydrogels showed a peak at 601 nm, which was red-shifted compared to the free QDs in solution. The phenomenon of red-shifting was also observed when QDs were dissolved in water at high concentrations (Supplementary Information Figure S1), likely due to fluorescence resonance energy transfer (FRET) occurring between QDs with variable sizes. When the QDs were entrapped in silk

hydrogels, the effect of FRET might have become more pronounced due to the proximity of the QDs to each other. The emission maximum was even more red-shifted with increased amounts of QDs in the hydrogels (Supplementary Information Figure S2). For both silk and silk/QDs hydrogels, the gelation time was about 30 min and the hydrogels were readily injectable through 18G needles. The fluorescence spectra of the silk/QDs microspheres were recorded and as shown in Figure 1B, the spectra did not change before and after QDs incorporation; both had emission maxima at 380 nm. The density of QDs in silk microspheres was not as high as in hydrogels, as a part of the QDs were washed away during microsphere preparation, as seen in the fluorescence images in Figure 1 A and B. Thus, no FRET took place in the silk microspheres, resulting in similar fluorescence spectra to the free QDs in solution (Figure 1B).

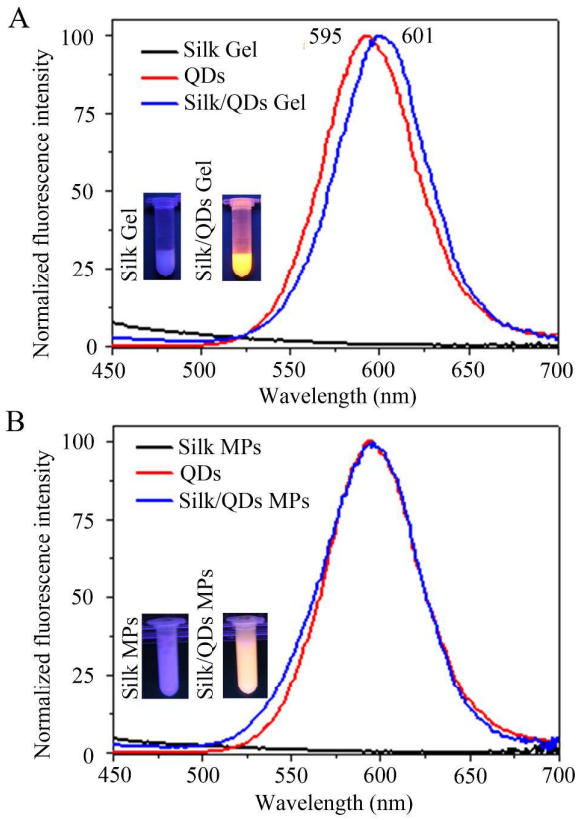

Figure 1. UV–Vis absorbance and fluorescence spectra of free QDs and QDs-incorporated silk hydrogels (A) and microspheres (B). The QDs loading in both hydrogels and microspheres was 0.065 nmol/mg silk.

3.2 Impact of QDs on structure and morphology of silk hydrogels and microspheres

FTIR was used to characterize the secondary structures. The characteristic absorption bands of silk in the Amide I (1595–1705 cm^{-1}) region are normally assigned to random coils, alpha–helices, β–pleated sheets and turns [19, 30, 31]. The absorption bands in the frequency range of 1616–1637 cm^{-1} and 1697–1703 cm^{-1} represent enriched β–sheet structures in silk [19, 30]. The absorption bands in the frequency range of 1638–1655 cm^{-1} were ascribed to random coil, 1656–1662 cm^{-1} to alpha–helices and 1663–1696 cm^{-1} to turns. In the present study, the bands shown at 1629 cm^{-1} and 1520 cm^{-1} indicated the formation of β–sheet structure in silk hydrogels (Figure 2A), consistent

with our previous results [32]. When QDs were loaded in silk hydrogels, with the increase of loading (0.013, 0.026, 0.065, 0.13, 0.26 nmol/mg silk) the absorption peak shifted from 1629 cm^{-1} to 1635 cm^{-1}, likely due to the influence of QDs on the absorption peak at 1635 cm^{-1}(Figure 2A). The peaks in Amide I region was deconvoluted and the contents of α-helices and β–sheets were shown in Figure S3. The bands positioned at 1616-1637 cm^{-1} and 1697-1703 cm^{-1} were assigned to β-sheet conformation, while that at 1638-1655 cm^{-1} to random coils, 1656-1662 cm^{-1} to helices, 1663-1696 cm^{-1} to β–turns [33]. The β–sheet structure contents calculated were 37.72, 34.59, 37.40, 40.61, 35.57, and 36.85 for silk hydrogels with loading of 0, 0.013, 0.026, 0.065, 0.13, and 0.26 nmol QDs per mg silk, respectively. The difference between samples was not significant ($p > 0.05$), indicating QDs incorporation in the silk hydrogels did not significantly influence silk β–sheet structure formation. Figure 2B showed the FTIR spectra of silk microspheres and QDs-incorporated microspheres. Compared with silk hydrogels, the absorption peaks of microsphere samples were broader, ranging from 1630 to more than 1656 cm^{-1}. These data are in agreement with our previous study [19], indicating that β–sheet structure formed in silk microspheres; the incorporation of QDs did not significantly change the structure of the silk.

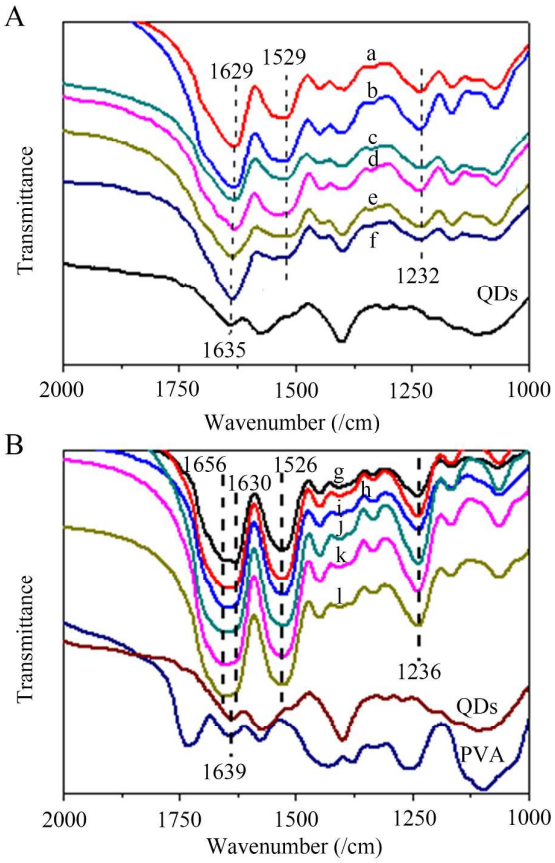

Figure 2. FTIR analyses on silk/QDs hydrogels (A) and microspheres (B). A, samples a-f were plain silk hydrogel and silk hydrogels loaded with 0.013, 0.026, 0.065, 0.13, 0.26 nmol/mg silk QDs, respectively. B, samples g-l were plain silk microspheres and silk microspheres loaded with loaded with 0.013, 0.026, 0.065, 0.13, 0.26 nmol/mg silk QDs, respectively.

The surface morphology of silk and silk/QDs hydrogels after lyophilization was examined by SEM (Figure 3). Silk hydrogels showed a porous structure with pore sizes approximately 1 μm with randomly orientated fibers and laminar layers, consistent with the literature [32]. Incorporation of QDs with low and high loading (0.026 and 0.26 nmol QDs per mg silk, respectively) did not change the morphology (Figure 3). Similarly, incorporation of QDs in silk microspheres did not change the

size and morphology of silk microspheres (Figure S4).

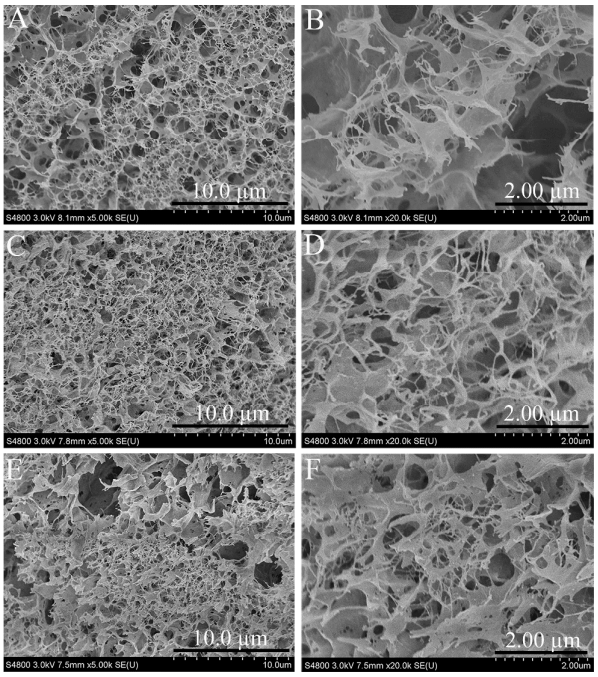

Figure 3. Silk hydrogel morphologies determined by SEM. A, D, silk hydrogel. B, E, silk/QDs hydrogel with low QDs loading (0.026 nmol/mg silk). C, F, silk/QDs hydrogel with high QDs loading (0.26 nmol/mg silk). Bar = 10 µm in A-C; 2 µm in D-F.

TEM was used to assess the encapsulation of QDs in the silk hydrogel matrix (Figure 4). The blank silk hydrogel displayed a homogeneous grey image under TEM (Figure 4A-C), while the QDs-loaded hydrogels showed evenly distributed dark spots throughout the gel matrix (Figure 4D-F). Incorporation of QDs in silk microspheres increased the dark density of silk/QDs microspheres when compared to the control of blank silk microspheres (Figure S5). Individual QDs could not be identified in this case due to the thickness (diameter 500-1000 nm) of the microspheres.

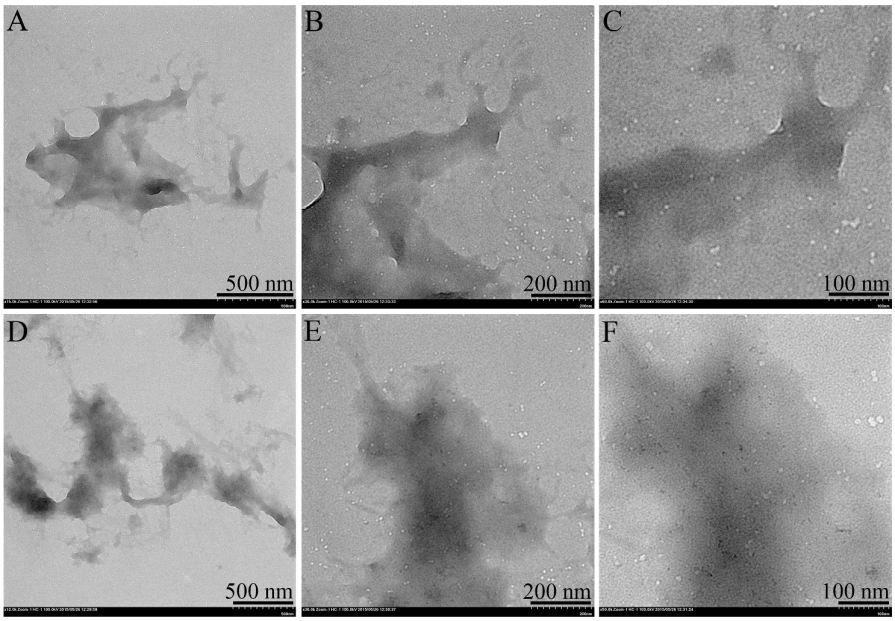

Figure 4. TEM images of silk and silk/QDs hydrogel. A-C: silk hydrogel. D-F: silk/QDs hydrogel with high QDs loading (0.13 mol per mg silk).

3.3 Stability of QDs in silk hydrogels and microspheres

3.3.1 Entrapment of QDs in silk hydrogel and microspheres

For *in vivo* optical imaging, QDs need to be tightly entrapped in silk biomaterials with minimal release in solution. An *in vitro* release experiment was conducted for QDs-incorporated silk hydrogels and microspheres, similar to the determination of drug release from silk biomaterials [34]. The amount of QDs in the release medium was calculated using a standard curve of QDs (Figure S6). As shown in Figure 5A, the entrapment of QDs was dependent on QDs loading in silk hydrogels; less QDs were released with decreased loading. When the QDs loading were 0.065, 0.13 and 0.26 nmol/mg silk, the release was 26.55% ± 0.085, 14.66% ± 1.1 and 12.00 % ± 0.16 of the total amount of QDs, respectively (Figure 5A insert), significantly higher than those with lower QDs loadings (0.013 and 0.026 nmol/mg silk) ($p < 0.05$). When the loading decreased to 0.026 μmol per mg silk or lower, the release of QDs was not detectable, indicating the QDs were bound to silk. The release kinetics of QDs was

non-linear. No release of QDs was detected in the first 10 min, and the level gradually increased with time and peaked at 12 hr (Figure 5B). After 12 hr, the level of fluorescence slowly decreased until reaching background (Figure 5B). For silk/QDs microspheres, release of QDs was not detectable during washing even at high loading (0.26 nmol mg silk). This was likely because the loosely associated QDs in the microspheres had been washed away during microsphere preparation.

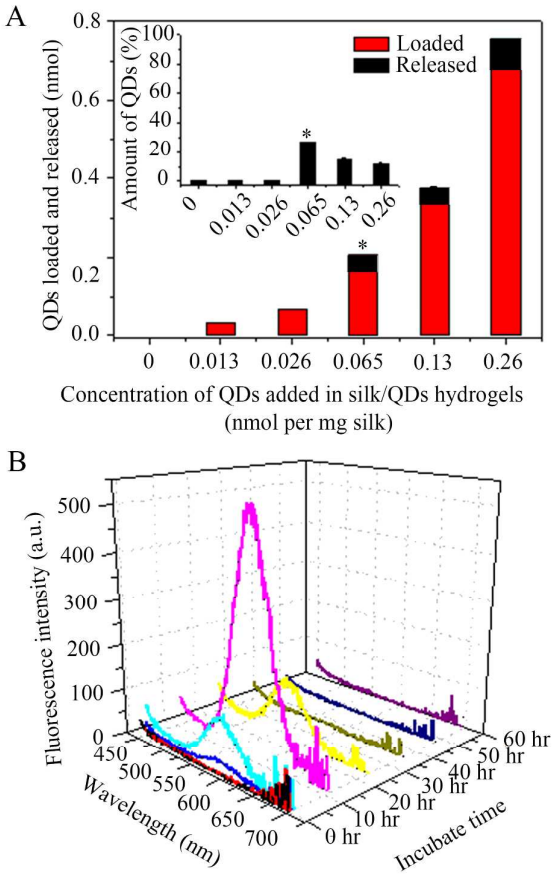

Figure 5. Relationship between QDs loading and entrapment in silk/QDs hydrogels (A), and fluorescence spectra of the release media from QDs-incorporated hydrogel (B). The loading of QDs in silk hydrogel in B was 0.13 nmol/mg silk. The release medium (1 mL) was replaced at 10, 60, 120 min, 12, 36, 60 hr. The amount of released QDs in 0.065 μmol/mg silk sample was significantly higher than those with lower QDs loading ($p < 0.05$).

3.3.2 Fluorescence stability of QDs in silk hydrogel and microspheres

The stability of QDs fluorescence is another important factor to consider when QDs are used as fluorescence probes for monitoring biomaterials. Silk/QDs hydrogels and microspheres were exposed to different solution environments and the change of fluorescence properties was determined in time (Figure 6). The fluorescence intensity of QDs continuously decreased accompanied by a blue shift of emission maximum in water, while it remained relatively stable in PBS within 96 hr at room temperature (Figure 6A-C). When the samples were incubated in PBS at different temperatures (4°C, room temperature, 37°C), the trend of change in QDs fluorescence was similar (Figure 6D). Figure S7 showed the influence of solution conditions and temperature on the fluorescence of QDs (Figure S7 A,C,E) and QDs incorporated in silk microspheres (Figure S7 B,D,F). In general, ionic conditions (water vs. PBS) and incubation temperature did not significantly influence QDs fluorescence in either free form in solution or entrapped form in microspheres.

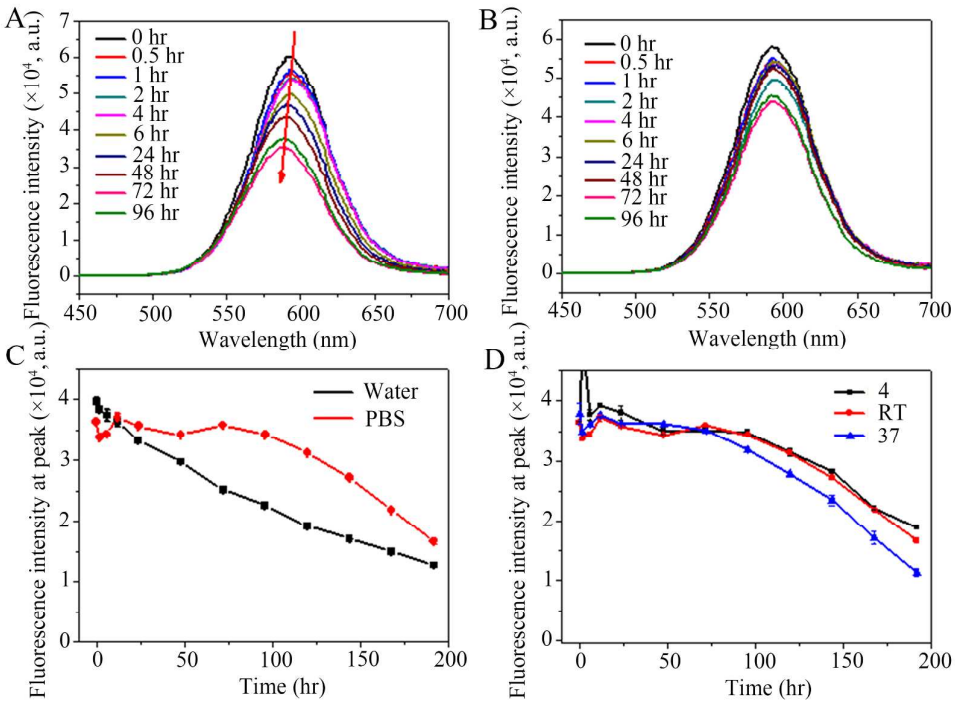

Figure 6. Influence of solution condition and temperature on the fluorescence of QDs incorporated in silk hydrogels. Silk/QDs hydrogel samples were incubated in water (A) or PBS (B) at 4°C, room temperature and 37°C. The loading of QDs in silk hydrogel was 0.13 nmol/mg silk.

3.4 Cytotoxicity study

The cytotoxicity of CdTe QDs has been reported, including impact on reproduction, regeneration, cell proliferation, and exerted genotoxicity [35]. To evaluated the cytotoxicity of QDs incorporated in silk biomaterials, human dermal fibroblasts (Hs 865.Sk cells) were cultured in the presence of silk/QDs hydrogel and microspheres and viability determined by CCK-8 assay. Figure 7 indicates that blank (control) silk hydrogels had little impact on cell survival, while the influence of silk/QDs hydrogels was QDs-concentration-dependent. Cells cultured with silk and silk/QDs hydrogels grew within 48hr, with low loading gels (0.013, 0.026 nmol/mg silk) supporting more proliferation than high loaded gels (0.065, 0.13 nmol/mg silk) at 48 hr (Figure 7). However, when equivalent doses of free QDs were added to the culture medium, cell

viability significantly decreased when compared to the silk/QDs hydrogel samples, indicating incorporation of QDs in silk hydrogels significantly attenuated the cytotoxicity of CdTe QDs. Similarly, incorporation of QDs in silk microspheres also reduced the cytotoxicity of CdTe QDs (Figure S8).

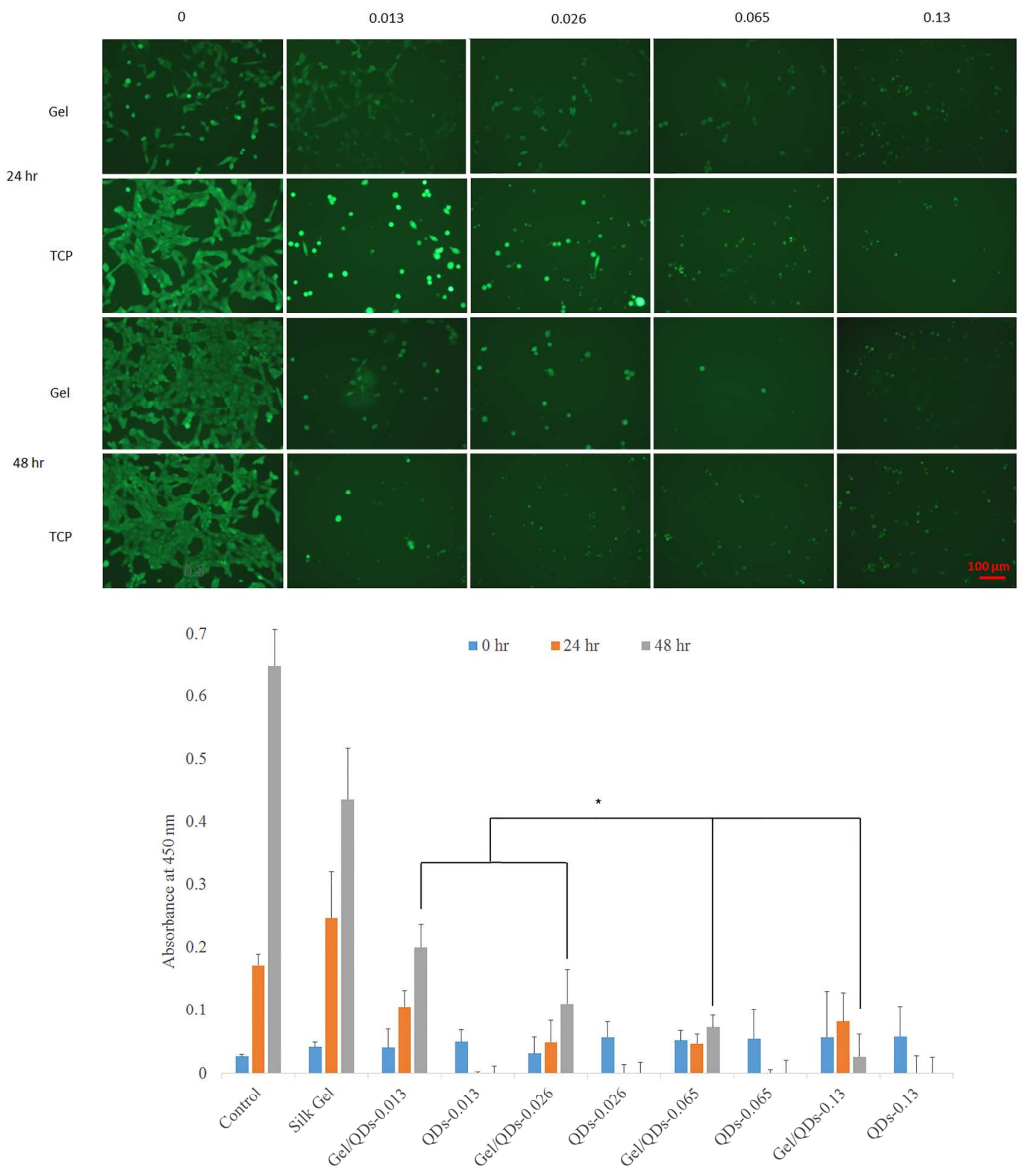

Figure 7. Human fibroblast cells (HS-865-SK) culture on sonication-induced plain silk hydrogels and silk hydrogels loaded with QDs (0.013, 0.026, 0.065, 0.13 nmol/mg silk QDs). QDs and empty wells (no materials) served as controls. The upper pictures show microscopic images taken for the cells at 24 and 48 hr after cells were exposed to the medium containing the test materials. The scale bar in the upper images is 100 μm. The lower graph shows the viability of cells determined by CCK-8 kit. Data shown as mean±SD, n=6; *$p<0.05$.

3.5 *In vivo* fluorescence imaging on silk/QDs hydrogel and microspheres

In vivo animal imaging was performed to track subcutaneously injected silk/QDs hydrogels and microspheres on the back of mice. The images were taken at an excitation wavelength of 500 nm and emission wavelength from 575 to 650 nm (DsRed) (Figure 8). Free QDs showed strong fluorescence under the skin after injection, but decreased quickly (QDs group in Figure 8 D,H,L). Fluorescence was completely quenched within 24 hr post injection. This was similar to the QDs incorporated silk microspheres, in which the fluorescence decreased quickly (Figure 8 B,F,J). The fluorescence of free QDs as the contral for silk/QDs microspheres was also quenched within 24 hr (data not shown). The fluorescence from the silk/QDs hydrogels remained stable over 96 hr (Figure 8). The control sample of plain silk hydrogels and microspheres and all the samples under bright field did not fluoresce. Thus, the fluorescence properties of QDs were protected by the silk hydrogels but not the microspheres in the *in vivo* environment, unlike the *in vitro* results. This finding was likely due to some of the microspheres diffusing away from the site of injection, even though weak fluorescence was still visible at the injection site after opening the skin (Figure 8J). Alternatively factors from the surrounding tissues penetrated into microspheres more easily than the hydrogels and caused fluorescence quenching.

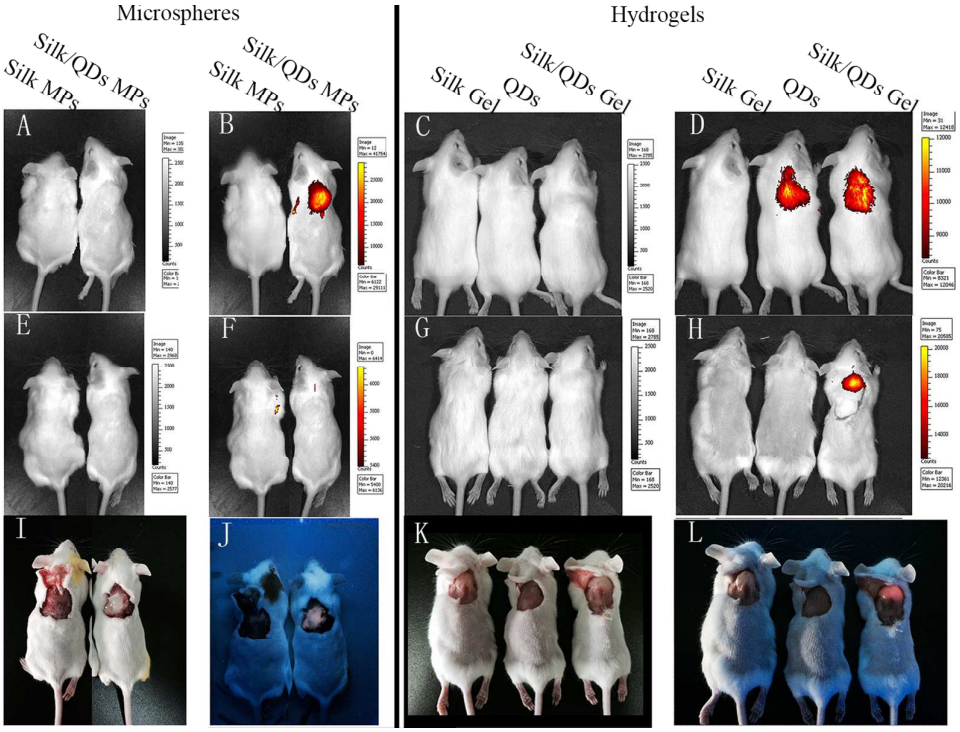

Figure 8. In vivo fluorescence imaging of subcutaneously injected silk/QDs microspheres and hydrogels for 24 hr. The QDs loading was 0.065 nmol/mg silk in microspheres and hydrogels. The images were taken under the bright field (A,E,I and C,G,K) and fluorescence field (B,F,J and D,H,L). A-D, images taken right after injection. E-H, images taken after 24 hr. I-L, the skin was cut open to expose the injected materials after 24 hr.

The fluorescence signal from silk/QDs hydrogels was further monitored for a longer period of time after injection (4 days) (Figure 9). The fluorescence decreased in the first 24 hr, and remained relatively stable (~30% of original fluorescence) until 96 h. The rapid decrease of fluorescence at the beginning may be due to the quenching of QDs located near the surface of the silk hydrogel, while those entrapped inside the gel matrix and strongly attached to the silk crystalline beta-sheet regions were protected from quenching. Relatively stable fluorescence signal from silk hydrogels should

permit further studies of biodegradation and metabolism of degradation products. The system established in the study could also be considered for implantable biosensing systems, for *in vivo* monitoring of diseases, such as for continuous glucose monitoring and related needs [36].

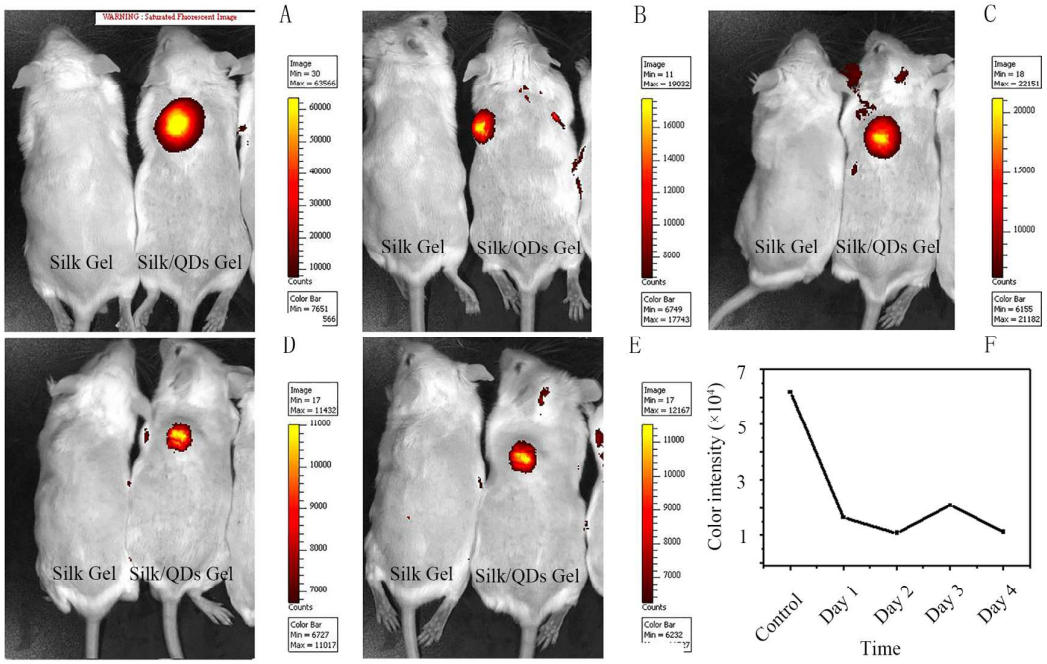

Figure 9. In vivo fluorescence imaging of subcutaneously injected silk/QDs hydrogel for 96 hr. A–D, images were taken at 0-4 days post injection. The mice were injected with silk hydrogels (left) and silk/QDs hydrogels (right). E, plot of fluorescence intensities from the silk/QDs hydrogel samples.

4 Conclusions

QDs were successfully incorporated into silk biomaterials via physical adsorption and entrapment, dependent on the mass ratio between the QDs and silk. The fluorescence of the QDs remained stable for more than 96 hr in silk hydrogels when immersed in PBS buffer, pH 7.4 (*in vitro*) or subcutaneously injected in mice. These time frames were significantly longer than that in silk microspheres (< 24 hr *in vitro*=). The

clearance of microspheres from the injection site or the rapid penetration of quenching factors into the microspheres from the surrounding tissues may account for the rapid quenching. The cytotoxicity of QDs was significantly reduced when the QDs were incorporated in silk hydrogels and microspheres. The QDs-incorporated silk hydrogels and microspheres with stable and strong fluorescence may be useful for tracking the degradation and distribution of silk biomaterials, as well as a potential diagnostic tool.

5. Acknowledgements

This work was supported by Natural Science Foundation of China grant (project no. 51273138 and 51403144), Start-up Fund of Soochow University (project no. 14317432), US NIH P41 EB002520, Natural Science Foundation of Suzhou City Jiangsu Province China (Grants No SYN201403), and Postdoctoral Science Foundation of Jiangsu Province China.

6. Statement of approval of animal experiments

The animal experiments shown in this study were approved and supervised by the ethical committee of Soochow University, China.

References

1. S. Hofmann, C. T. W. P. Foo, F. Rossetti, M. Textor, G. Vunjak-Novakovic, D. L. Kaplan, H. P. Merkle and L. Meinel, *J Control Release*, 2006, **111**, 219-227.
2. Y. Z. Wang, H. J. Kim, G. Vunjak-Novakovic and D. L. Kaplan, *Biomaterials*, 2006, **27**, 6064-6082.
3. T. Yucel, M. L. Lovett and D. L. Kaplan, *J Control Release*, 2014, **190**, 381-397.
4. N. Minoura, S. I. Aiba, M. Higuchi, Y. Gotoh, M. Tsukada and Y. Imai, *Biochem Bioph Res Co*, 1995, **208**, 511-516.
5. F. Wang, C. Yang and X. Hu, eds. Y. Yang, H. Xu and X. Yu, American Chemical Society, 2014, pp. 177-208.
6. D. N. Rockwood, R. C. Preda, T. Yucel, X. Q. Wang, M. L. Lovett and D. L. Kaplan, *Nat Protoc*, 2011, **6**, 1612-1631.
7. X. Michalet, F. F. Pinaud, L. A. Bentolila, J. M. Tsay, S. Doose, J. J. Li, G. Sundaresan, A. M. Wu, S. S. Gambhir and S. Weiss, *Science*, 2005, **307**, 538-544.
8. L. A. Bentolila, Y. Ebenstein and S. Weiss, *J Nucl Med*, 2009, **50**, 493-496.
9. U. Resch-Genger, M. Grabolle, S. Cavaliere-Jaricot, R. Nitschke and T. Nann, *Nat Methods*, 2008, **5**, 763-775.
10. B. Dubertret, P. Skourides, D. J. Norris, V. Noireaux, A. H. Brivanlou and A.

Libchaber, *Science*, 2002, **298**, 1759-1762.
11. F. Ye, A. Barrefelt, H. Asem, M. Abedi-Valugerdi, I. El-Serafi, M. Saghafian, K. Abu-Salah, S. Alrokayan, M. Muhammed and M. Hassan, *Biomaterials*, 2014, **35**, 3885-3894.
12. K. Li, D. Ding, D. Huo, K. Y. Pu, N. P. T. Ngo, Y. Hu, Z. Li and B. Liu, *Adv Funct Mater*, 2012, **22**, 3107-3115.
13. Y. Guo, D. L. Shi, H. S. Cho, Z. Y. Dong, A. Kulkarni, G. M. Pauletti, W. Wang, J. Lian, W. Liu, L. Ren, Q. Q. Zhang, G. K. Liu, C. Huth, L. M. Wang and R. C. Ewing, *Adv Funct Mater*, 2008, **18**, 2489-2497.
14. M. G. Panthani, T. A. Khan, D. K. Reid, D. J. Hellebusch, M. R. Rasch, J. A. Maynard and B. A. Korgel, *Nano Lett*, 2013, **13**, 4294-4298.
15. B. B. Nathwani, M. Jaffari, A. R. Juriani, A. B. Mathur and K. E. Meissner, *Ieee T Nanobiosci*, 2009, **8**, 72-77.
16. S. Q. Chang, Y. D. Dai, B. Kang, W. Han and D. Chen, *J Nanosci Nanotechno*, 2009, **9**, 5693-5700.
17. H. L. Su, J. Han, Q. Dong, D. Zhang and Q. X. Guo, *Nanotechnology*, 2008, **19**.
18. X. Q. Wang, J. A. Kluge, G. G. Leisk and D. L. Kaplan, *Biomaterials*, 2008, **29**, 1054-1064.
19. X. Q. Wang, T. Yucel, Q. Lu, X. Hu and D. L. Kaplan, *Biomaterials*, 2010, **31**, 1025-1035.
20. V. Gupta, A. Aseh, C. N. Rios, B. B. Aggarwal and A. B. Mathur, *Int J Nanomed*, 2009, **4**, 115-122.
21. S. Z. Lu, X. Q. Wang, Q. Lu, X. Hu, N. Uppal, F. G. Omenetto and D. L. Kaplan, *Biomacromolecules*, 2009, **10**, 1032-1042.
22. X. Q. Wang, E. Wenk, X. H. Zhang, L. Meinel, G. Vunjak-Novakovic and D. L. Kaplan, *J Control Release*, 2009, **134**, 81-90.
23. S. S. Silva, A. Motta, M. T. Rodrigues, A. F. M. Pinheiro, M. E. Gomes, J. F. Mano, R. L. Reis and C. Migliaresi, *Biomacromolecules*, 2008, **9**, 2764-2774.
24. M. Demura and T. Asakura, *Biotechnol Bioeng*, 1989, **33**, 598-603.
25. N. Gaponik, D. V. Talapin, A. L. Rogach, K. Hoppe, E. V. Shevchenko, A. Kornowski, A. Eychmuller and H. Weller, *J Phys Chem B*, 2002, **106**, 7177-7185.
26. S. Kaniyankandy, S. Rawalekar, S. Verma, D. K. Palit and H. N. Ghosh, *Phys Chem Chem Phys*, 2010, **12**, 4210-4216.
27. C. Li, C. Vepari, H. J. Jin, H. J. Kim and D. L. Kaplan, *Biomaterials*, 2006, **27**, 3115-3124.
28. F. Denizot and R. Lang, *J Immunol Methods*, 1986, **89**, 271-277.
29. W. W. Yu, L. H. Qu, W. Z. Guo and X. G. Peng, *Chem Mater*, 2003, **15**, 2854-2860.
30. A. Vasconcelos, G. Freddi and A. Cavaco-Paulo, *Biomacromolecules*, 2008, **9**, 1299-1305.
31. X. Chen, D. P. Knight and Z. Shao, *Soft Matter*, 2009, **5**, 2777-2781.
32. X. Wang, B. Partlow, J. Liu, Z. Zheng, B. Su, Y. Wang and D. L. Kaplan, *Acta*

biomaterialia, 2015, **12**, 51-61.
33. X. Hu, D. Kaplan and P. Cebe, *Macromolecules*, 2006, **39**, 6161-6170.
34. E. M. Pritchard and D. L. Kaplan, *Expert opinion on drug delivery*, 2011, **8**, 797-811.
35. A. Ambrosone, L. Mattera, V. Marchesano, A. Quarta, A. S. Susha, A. Tino, A. L. Rogach and C. Tortiglione, *Biomaterials*, 2012, **33**, 1991-2000.
36. Y. J. Heo, H. Shibata, T. Okitsu, T. Kawanishi and S. Takeuchi, *P Natl Acad Sci USA*, 2011, **108**, 13399-13403.

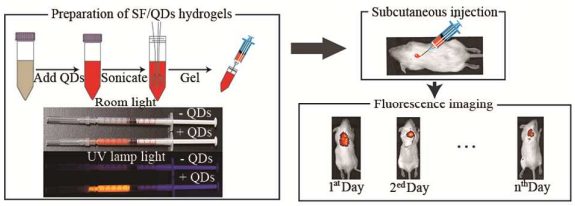
Preparation of SF/QDs hydrogels
Add QDs
Sonicate
Gel
Room light
- QDs
+ QDs
UV lamp light
- QDs
+ QDs
Subcutaneous injection
Fluorescence imaging
1st Day
2ed Day
...
nth Day